Density Functional Characterization of Reactions of Bimetallic Carbenes $PtMCH_2^+$ (M = Pt, Au) with NH_3 in the Gas Phase

Fei Xia, Jian Chen, Kuo Zeng, and Zexing Cao*

Department of Chemistry, State Key Laboratory of Physical Chemistry of Solid Surfaces, Xiamen University, Xiamen 361005, China

Received November 22, 2004

Dehydrogenation and C−N coupling from $PtMCH_2^+$ (M = Pt, Au) and ammonia have been investigated by the density functional methodology. The structure and stability of intermediates and ionic products as well as detailed mechanisms for loss of H_2 and degradation of the metal core have been discussed. Calculations reveal that in the case of $Pt_2CH_2^+$ only direct elimination of H_2 from the moiety of CH_2 occurs in the adduct $(NH_3)Pt_2CH_2^+$, and the activation energy for the rate-determining step is about 30 kcal mol^{-1}. The overall reaction is exothermic by ~30 kcal mol^{-1}. The heterometallic carbene $PtAuCH_2^+$ exhibits reactivity different from $Pt_2CH_2^+$. The dehydrogenation from C−H and NH_3 activation can occur in competitive mechanisms, where the channel to loss of H_2 from the stepwise N−H and C−H activation is more favorable than the elimination of H_2 in methylene or in NH_3 both thermodynamically and dynamically. The ionic product aminocarbene $AuPtCHNH_2^+$ reacts with NH_3, giving rise to the loss of H_2 and AuH. Predicted relative energetics and barriers along suggested reaction paths are in reasonable agreement with experimental observations. Different reactivities of $PtAuCH_2^+$ and $Pt_2CH_2^+$ in the gas-phase reactions with NH_3 arise from distinct geometrical and electronic structures of their reactive precursors.

Introduction

Methane is a facile source for synthesis of hydrocarbons, and its activation and functionalization are of fundamental importance in organometallic, biological, and industrial chemistry.[1] Due to the high stability of C−H bonds, the catalytic conversion of methane into industrially important derivatives generally is difficult to achieve. The utilization of transition metal centers has been demonstrated to be one of the feasible approaches.[2] In particular, the platinum catalyst highlights its importance in the selective oxidation of methane.[3] Quite a number of experimental and theoretical investigations on gas-phase reactions of methane with transition metal ions have been implemented.[4]

Platinum as a heterogeneous catalyst can catalyze C−N bond coupling of ammonia and methane at high temperatures according to reaction 1. Although this

$$CH_4 + NH_3 \rightarrow HCN + 3H_2 \qquad (1)$$

process has been used for the large-scale synthesis of hydrogen cyanide, the detailed mechanism of the heterogeneous process is still unclear.[5] Under the circumstances, gas-phase studies can provide essential information on the elementary steps for the cleavage and formation of bonds as well as intermediates. Aschi et al.[6] explored the Pt^+-catalyzed C−N bond coupling of methane and ammonia on the $Pt^+/CH_4/NH_3$ model system using the technology of Fourier transform ion cyclotron resource (FTICR) mass spectrometry.[7] They found that the cationic platinum carbene $PtCH_2^+$, originating from the dehydrogenation of methane mediated by the bare platinum cation, can react rapidly with ammonia to give products $CH_2NH_2^+$, $PtC(H)NH_2^+$, and NH_4^+ in a ratio of 70:25:5 according to reactions 2a−2c:

$$PtCH_2^+ + NH_3 \rightarrow CH_2NH_2^+ + PtH \qquad (2a)$$

$$PtCH_2^+ + NH_3 \rightarrow PtC(H)NH_2^+ + H_2 \qquad (2b)$$

$$PtCH_2^+ + NH_3 \rightarrow NH_4^+ + PtCH \qquad (2c)$$

In reactions 2a and 2b, C−N bond coupling is involved. The mechanism of proton transfer is demonstrated by deuterium labeling and collision-induced

* Corresponding author. E-mail: zxcao@xmu.edu.cn.

(1) (a) Crabtreee, R. H. *Chem. Rev.* **1995**, *95*, 987. (b) Lunsford, J. H. *Angew. Chem.* **1995**, *107*, 1059; *Angew. Chem., Int. Ed. Engl.* **1995**, *43*, 970.

(2) (a) Labinger, J. A.; Bercaw, J. E. *Nature* **2002**, *417*, 507. (b) Schwarz, H.; Schröder, D. *Pure Appl. Chem.* **2000**, *72*, 2319.

(3) Periana, R. A.; Taube, D. J.; Gamble, S.; Taube, H.; Satoh, T.; Fujii, H. *Science* **1998**, *280*, 560.

(4) (a) Irikura, K. K.; Beauchamp, J. L. *J. Am. Chem. Soc.* **1989**, *111*, 75. (b) Irikura, K. K.; Beauchamp, J. L. *J. Am. Chem. Soc.* **1991**, *113*, 2769. (c) Irikura, K. K.; Beauchamp, J. L. *J. Phys. Chem.* **1991**, *95*, 8344. (d) Wesendrup, R.; Schröder, D.; Schwarz, H. *Angew. Chem., Int. Ed. Engl.* **1994**, *33*, 1174. (e) Heinemann, C.; Wesendrup, R.; Schwarz, H. *Chem. Phys. Lett.* **1995**, *239*, 75. (f) Pavlov, M.; Blomberg, M. R. A.; Siegbahn, P. E. M.; Wesendrup, R.; Heinemann, C.; Schwarz, H. *J. Phys. Chem. A* **1997**, *101*, 1567.

(5) (a) Hasenberg, D.; Schmidt, L. D. *J. Catal.* **1985**, *91*, 116. (b) Hasenberg, D.; Schmidt, L. D. *J. Catal.* **1986**, *97*, 156. (c) Hasenberg, D.; Schmidt, L. D. *J. Catal.* **1987**, *104*, 441. (d) Waletzko, N.; Schmidt, L. D. *AlChE J.* **1988**, *34*, 1146. (e) Bockholt, A.; Harding, I. S.; Nix, R. M. *J. Chem. Soc., Faraday Trans.* **1997**, *93*, 3869.

(6) Aschi, M.; Brönstrup, M.; Diefenbach, M.; Jeremy, N. H.; Schröder, D.; Schwarz, H. *Angew. Chem., Int. Ed.* **1998**, *37*, 829.

(7) (a) Eller, K.; Schwarz, H. *Int. J. Mass Spectrom. Ion Processes* **1989**, *93*, 243. (b) Eller, K.; Zummack, W. *J. Am. Chem. Soc.* **1990**, *112*, 621. (c) Eller, K.; Schwarz, H. *Chem. Rev.* **1991**, *91*, 1121.

10.1021/om0490942 CCC: $30.25
Publication on Web 03/08/2005

dissociation (CID) experiments.[6,8] For the mononuclear cationic metal carbene $PtCD_2^+$, it reacts with ammonia to yield $CD_2NH_2^+$ and PtH as the main channel. The loss of PtH apparently indicates the activation of ammonia. In reaction 2b, HD loss is observed exclusively and the formation of the aminocarbene structure $PtC(D)NH_2^+$ indicates that the hydrogen elimination can occur at carbon and nitrogen atoms, respectively. The aminocarbene $PtC(D)NH_2^+$ reacts with a second NH_3 to yield HD and possible biaminocarbene ion complex $PtC(NH_2)_2^+$.[6] In combination with primary density functional calculations, possible structures of the species in the Pt^+-catalyzed coupling of methane and ammonia are suggested.[8a]

Recently, Koszinowski et al.[9a] studied the cooperative effects of bimetallic clusters Pt_2^+ and $PtAu^+$ on the C−N coupling of CH_4 and NH_3. The heterometallic carbene $PtAuCH_2^+$ reacts with NH_3 to result in the loss of H_2 according to reaction 3. The ionic product $[Pt,Au,C,H_3,N]^+$ undergoes consecutive reactions (4 and 5) in the presence of NH_3 to produce H_2 or AuH.

$$PtAuCH_2^+ + NH_3 \rightarrow [Pt,Au,C,H_3,N]^+ + H_2 \quad (3)$$

$$[Pt,Au,C,H_3,N]^+ + NH_3 \rightarrow [Pt,Au,C,H_4,N_2]^+ + H_2 \quad (4)$$

$$\rightarrow [Pt,C,H_5,N_2]^+ + AuH \quad (5)$$

Experimental observations indicate that $PtAu^+$ has a reactivity similar to Pt^+ and it mediates the dehydrogenation and C−N coupling from methane and ammonia. Unlike Pt^+ and $PtAu^+$, Pt_2^+ and small cationic platinum clusters do not mediate C−N coupling from CH_4 and NH_3; rather, they dehydrogenate methane and ammonia and form the adduct of the ion product with a second NH_3 according to reactions 6a−6c.[9b]

$$Pt_n^+ + CH_4 \rightarrow Pt_nCH_2^+ + H_2 \quad (6a)$$

$$Pt_nCH_2^+ + NH_3 \rightarrow [Pt_n,C,N,H_3]^+ + H_2 \quad (6b)$$

$$[Pt_n,C,N,H_3]^+ + NH_3 \rightarrow [Pt_n,C,N_2,H_6]^+ \quad (6c)$$

Despite all these important contributions, the detailed mechanisms for coupling of methane and ammonia mediated by bimetallic clusters remain open.[9c] In the present work, we performed extensive density functional calculations to elucidate the mechanistic details for the C−N coupling and dehydrogenation mediated by bimetallic carbene cations. Plausible reaction channels and structures of intermediates, transition states, and products have been explored.

Computational Details

All calculations have been performed by the Gaussian 98 package.[10] The hybrid B3LYP functional[11,12] was used to locate structures of stationary points on the potential energy surface (PES). The nature of minima and transition states on the PES was assessed by vibrational analyses. Geometry optimization and frequency calculations were carried out with the double-ζ basis set augmented by polarization functions. For nonmetal carbon, nitrogen, and hydrogen, the standard 6-31G* basis set was employed; the Lanl2dz basis set in combination with Hay and Wadt's relativistic effective core potential (ECP)[13,14] was used for Pt and Au atoms.

Relative energetics along the reaction channel were predicted by single-point energy calculations with the 6-311+G(3df,2df,2p) basis set for nonmetals and the Lanl2dz ECP basis set augmented with an f-polarization function[15] for transition metal atoms. The metal dimer $PtAu^+$ has been used to validate the reliability of the B3LYP functional. DFT calculations predict that the energy difference between the ground state $^1\Sigma^+$ and the excited triplet state $^3\Delta$ is 7 kcal mol^{-1}, which is intermediate between 9 kcal mol^{-1} by CCSD and 4.3 kcal mol^{-1} by CCSD(T). At the MRSDCI level,[16] the low-lying state $^3\Delta$ is higher in energy than the ground state by 4.7 kcal mol^{-1}. In previous theoretical investigations on the interaction of Pt_2/Pd_2 with H_2/CH_4, B3LYP calculations show good agreement with the sophisticated treatment.[17] Although the present calculations cannot predict accurately thermodynamic values due to significant relativistic effects in such heavy transition metal systems,[18] predicted thermochemical data may provide a reasonable basis for a mechanistic description of the gas-phase reactions of bimetallic carbene and ammonia.

Results and Discussion

I. Structures and Stabilities of the Dinuclear Metal Cationic Carbenes. Optimized geometries of stable isomers of bimetallic species $Pt_2CH_2^+$ and $AuPtCH_2^+$ and corresponding electronic states are displayed in Figure 1. B3LYP calculations show that the ground state $^2A_2$ of $Pt_2CH_2^+$ has an optimized structure **c** with C_{2v} symmetry, which is lower in energy than the isomer **a** ($^2A'$) by 19.0 kcal mol^{-1}. Pt−Pt and Pt−C bond lengths in the most stable structure **c** are

(8) (a) Diefenbach, M.; Aschi, M.; Schröder, D.; Schwarz, H. *J. Am. Chem. Soc.* **1999**, *121*, 10614. (b) Brunier, R. C.; Cody, R. B.; Freiser, B. S. *J. Am. Chem. Soc.* **1982**, *104*, 7436. (c) Cody, R. B.; Freiser, B. S. *Int. J. Mass Spectrom. Ion Phys.* **1982**, *41*, 199.

(9) (a) Koszinowski, K.; Schröder, D.; Schwarz, H. *J. Am. Chem. Soc.* **2003**, *125*, 3676. (b) Koszinowski, K.; Schröder, D.; Schwarz, H. *Organometallics* **2003**, *22*, 3819. (c) Koszinowski, K.; Schröder, D.; Schwarz, H. *Angew. Chem., Int. Ed.* **2004**, *43*, 121. (d) Koszinowski, K.; Schröder, D.; Schwarz, H. *Organometallics* **2004**, *23*, 1132. (e) Koszinowski, K.; Schlangen, M.; Schröder, D.; Schwarz, H. *Int. J. Mass Spectrum* **2004**, *23*, 19.

(10) Frisch, M. J.; Trucks, G. W.; Schlegel, H.B.; Scuseria, G. E.; Robb, M. A.; Cheeseman, J. R.; Zakrzewski, V. G.; Montgomery, J. A., Jr.; Stratmann, R. E.; Burant, J. C.; Dapprich, S.; Millam, J. M.; Daniels, A. D.; Kudin, K. N.; Strain, M. C.; Farkas, O.; Tomasi,; J.; Barone, V.; Cossi, M.; Cammi, R.; Mennucci, B.; Pomelli, C.; Adamo, C.; Clifford, S.; Ochterski, J.; Petersson, G. A.; Ayala, P. Y.; Cui, Q.; Morokuma, K.; Salvador, P.; Dannenberg, J. J.; Malick, D. K.; Rabuck, A. D.; Raghavachari, K.; Foresman, J. B.; Cioslowski, J.; Ortiz, J. V.; Baboul, A. G.; Stefanov, B. B.; Liu, G.; Liashenko, A.; Piskorz, P.; Komaromi, I.; Gomperts, R.; Martin, R. L.; Fox, D. J.; Keith, T.; Al-Laham, M. A.; Peng, C. Y.; Nanayakkara, A.; Challacombe, M.; Gill, P. M. W.; Johnson, B.; Chen, W.; Wong, M. W.; Andres, J. L.; Gonzalez, C.; Head-Gordon, M.; Replogle, E. S.; Pople, J. A. *Gaussian98*; Gaussian Inc.: Pittsburgh, PA, 1998.

(11) Becke, A. D. *J. Chem. Phys.* **1993**, *98*, 5648.

(12) Lee, C.; Yang, W.; Parr, R. G. *Phys. Rev. B* **1988**, *37*, 785.

(13) (a) Hay, P. J.; Wadt, W. R. *J. Chem. Phys.* **1985**, *82*, 270. (b) Hay, P. J.; Wadt, W. R. *J. Chem. Phys.* **1985**, *82*, 299.

(14) Wadt, W. R.; Hay, P. J. *J. Chem. Phys.* **1985**, *82*, 284.

(15) Ehlers, A. W.; Böhme, M.; Sapprich, S.; Gobbi, A.; Höllwarth, A.; Jonas, V.; Köhler, K. F.; Stegmann, R.; Veldkamp, A.; Grenking, G. *Chem. Phys. Lett.* **1993**, *208*, 111.

(16) Dai, D. G.; Balasubramanian, K. *J. Chem. Phys.* **1994**, *6*, 100.

(17) Cui, Q.; Djamaladdin, G.; Morokuma, K. J. *J. Chem. Phys.* **1998**, *108*, 8414.

(18) (a) Pyykkö, P. *Chem. Rev.* **1988**, *88*, 563. (b) Kaltsoyannis, N. J. *Chem. Soc., Dalton Trans.* **1996**, *1*, 1.

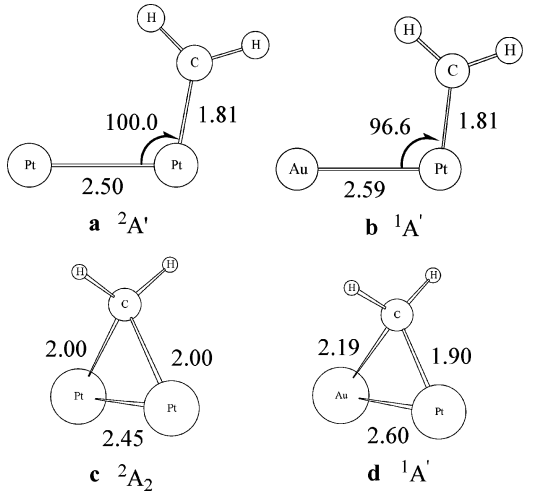

Figure 1. B3LYP-optimized structures of $Pt_2CH_2^+$ and $PtAuCH_2^+$ (bond lengths in angstroms and bond angles in degrees).

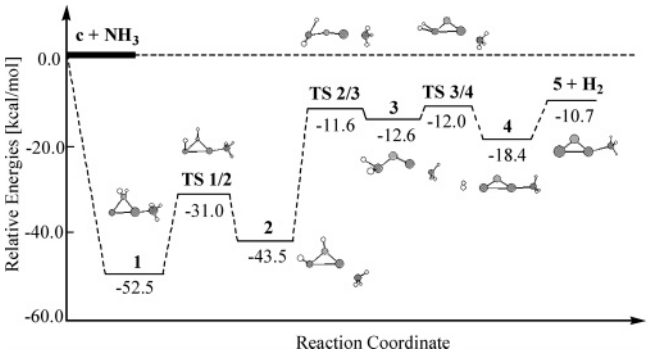

Figure 2. Doublet potential energy profiles along the pathway to loss of H_2 from the moiety of CH_2 in the reaction of $Pt_2CH_2^+$ with NH_3.

2.45 and 2.00 Å, respectively. In species **a**, NBO analysis reveals that the CPt bond has a character of a double bond, where the interaction between the hybrid sp^2 (C) and sd^2 (Pt) orbitals contributes the σ bonding and the p (C) and d (Pt) orbitals are responsible for the π bonding.

The heteronuclear bimetallic species, $AuPtCH_2^+$, derivated from the replacement of the terminal Pt atom in $Pt_2CH_2^+$, has similar stable structures **b** and **d**. In contrast to isomers of $Pt_2CH_2^+$, DFT calculations predict that isomers **b** and **d** of $AuPtCH_2^+$ are almost isoenergetic. The sp^3 carbon atom in **d** has a saturated tetrahedral structure different from **b**. The barrier for the conversion from **b** to **d** is only about 3 kcal mol^{-1}. Presumably, owing to such high stability of the isomer **c**, it should be the dominant precursor to reaction of $Pt_2CH_2^+$ with ammonia. For $AuPtCH_2^+$, both isomers **b** and **d** may be assumed as precursors reacting with ammonia, showing different reactivity from $Pt_2CH_2^+$ as observed in experiments.[9]

II. Reactions of $Pt_2CH_2^+$ with NH_3. Low-energy reaction channels of $Pt_2CH_2^+$ with NH_3, giving rise to loss of H_2, and corresponding energetics are shown in Figure 2, where the zero-point energies (ZPE) are included. Optimized structures of intermediates, transition states, and dehydrogenated products in the reaction are given in Figure 3. Table 1 collects selected thermodynamic values.

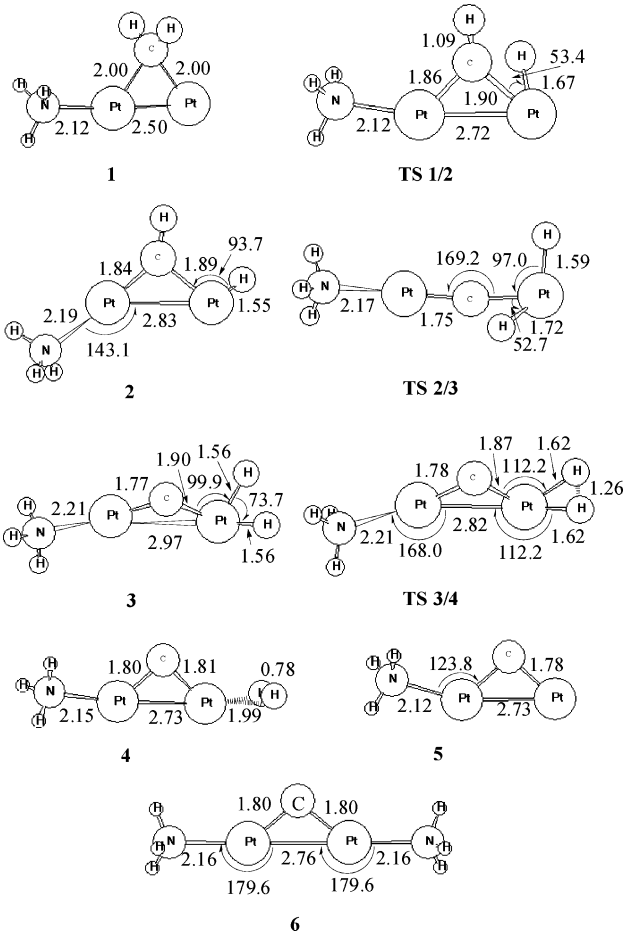

Figure 3. B3LYP-optimized structures of intermediates and transition states corresponding to Figure 2 (bond lengths in angstroms and bond angles in degrees).

As Figure 2 displays, coordination of NH_3 to the terminal Pt in **c** leads to complex **1** with the complexation energy of 52.5 kcal mol^{-1}. In complex **1**, the Pt−N bond length is 2.12 Å. NBO analyses indicate that strong donor−acceptor interactions (~56 kcal mol^{-1}) arising from a lone pair of NH_3 and an antibonding orbital of the Pt_2 subunit are responsible for the Pt−N bond. Complex **1** proceeds to an intermediate **2** through the transition state **TS 1/2** with a barrier of 21.5 kcal mol^{-1}. The consecutive hydrogen atom migration from carbon to Pt results in the dihydride **3** with a barrier of 31.9 kcal mol^{-1}. Both processes include cleavage of the strong C−H bond ($D_0(CH_3-H)$ = 103.4 kcal mol^{-1})[19] and formation of a relatively weak Pt−H bond ($D_0(Pt-H)$ = 74.0 kcal mol^{-1}),[20] and they are the rate-determining steps. Followed by dihydrogen formation, **3** evolves into a more stable intermediate **4** with a neglectable barrier. Finally, loss of H_2 in **5** requires ~8 kcal mol^{-1}.

Overall, the reaction 6b ($n = 2$) has an exothermicity of 10.7 kcal mol^{-1} and free energies of reaction ΔG of −12.5 kcal mol^{-1}(298.15 K). The dehydrogenation occurs only at CH_2, as shown in the isotopic labeling experiment for the homonuclear platinum cluster.[9b] The significant exothermicity for formation of the intermediate **1** may facilitate the loss of H_2 in the reaction. The dehydrogenated product **5** has a bridging-carbon struc-

(19) Litorja, M.; Ruscic, B. *J. Chem. Phys.* **1997**, *107*, 9852.
(20) Wittborn, C.; Wahlgren, U. *Chem. Phys.* **1995**, *201*, 357.

Table 1. Relative Energies and Thermodynamic Values (kcal mol^{-1}) of Selected Species in Reactions of $PtMCH_2^+$ with NH_3 by the B3LYP Approach

species	$\Delta E^a + \Delta ZPE$	$\Delta E + \Delta ZPE$	ΔH^0	ΔG^0
$Pt_2CD_2^+ + NH_3$	0.0	0.0	0.0	0.0
2	−43.5	−48.5	−48.8	−40.5
TS 2/3	−11.6	−12.4	−13.0	−3.8
5 + D_2	−10.7	−14.1	−13.1	−12.5
$AuPtCD_2^+ + NH_3$	0.0	0.0	0.0	0.0
loss of D_2				
7	−47.1	−53.15	−53.6	−44.8
TS 7/8	−15.3	−18.32	−19.3	−9.4
8	−45.6	−48.2	−49.0	−39.2
TS 8/9	−11.2	−7.6	−8.3	1.5
11 + D_2	8.6	5.58	6.7	7.1
loss of HD				
12	−43.7	−49.7	−50.3	−41.2
TS 12/14	−16.5	−22.5	−23.4	−13.7
14	−39.3	−42.9	−48.9	−37.9
TS 14/15	−16.1	−21.1	−22.6	−11.2
18 + HD	−30.2	−35.7	−35.3	−33.1
loss of H_2				
15	−50.4	−54.5	−55.9	−44.6
TS 15/20	−9.4	−13.8	−14.6	−4.6
20	−43.6	−47.5	−48.3	−38.3
TS 20/21	−34.6	−38.5	−39.4	−29.6
22 + H_2	−14.2	−20.5	−20.1	−18.0
$AuPtCHNH_2^+ + NH_3$	0.0	0.0	0.0	0.0
26	−25.7	−22.2	−23.0	−12.8
TS 26/27	−6.7	−5.3	−9.3	0.0
27	−20.2	−24.2	−25.0	−14.8
28 + H_2	−9.7	−14.6	−14.1	−11.6
19 + 29	5.2	0.5	6.4	0.8

[a] Relative energies from B3LYP calculations with the 6-311+G(3df,2df,2p) basis set for nonmetals and the Lanl2dz ECP basis set augmented with an f-polarization function at the optimized geometries with the basis sets of 6-31G* for nonmetal atoms and Lanl2dz ECP for transition metal atoms.

ture. The presence of the carbide moiety of Pt_2C^+ in the product **5** was confirmed by the collision-induced dissociation (CID) experiment.[9b] The coordination of a second NH_3 to **5** yields **6** with an exothermicity of 44.5 kcal mol^{-1}. Such high stability of **6** as well as the relatively coordinated saturated metal center makes the platinum site in these species less active and the consecutive reactions concerning NH_3 activation cannot occur as observed in experiments.[9] Predicted structures **5** and **6** can serve as candidates for the observed ion products $[Pt_2,C,N,H_3]^+$ and $[Pt_2,C,N_2,H_6]^+$ in experimental studies.[9a]

III. Reactions of $PtAuCH_2^+$ and NH_3. Isotopic labeling experiments demonstrate that the dehydrogenation reaction 3 of $PtAuCD_2^+$ with NH_3 yields a mixture of D_2, HD, and H_2 in a comparable ratio. This shows that both C−H and N−H activations can occur in the dehydrogenation reaction. Figures 4, 6, and 8 present possible mechanisms and relative energies for loss of D_2, HD, and H_2, respectively. Optimized geometries of intermediates and transition states are depicted in Figures 5, 7, and 9. Selected thermodynamic values are incorporated into Table 1.

Loss of D_2. Calculations reveal that the reaction of the isomer **b** with NH_3 undergoes a lower barrier than that of **d** with NH_3 in the dehydrogenation process. As a branch of reaction 3, the low-energy mechanistic scheme for loss of D_2 from the heteronuclear carbene $PtAuCD_2^+$ is shown in Figure 4. The terminal Au in $PtAuCD_2^+$ binds NH_3 with an exothermicity of 47.1 kcal

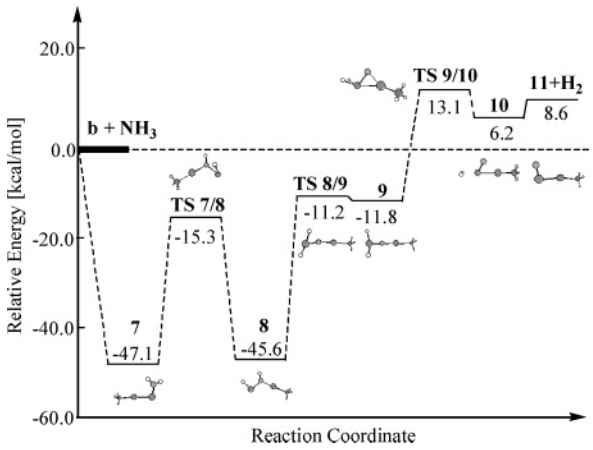

Figure 4. Singlet potential energy profiles along the pathway to loss of H_2 from the moiety of CH_2 in the complex $(NH_3)PtAuCH_2^+$.

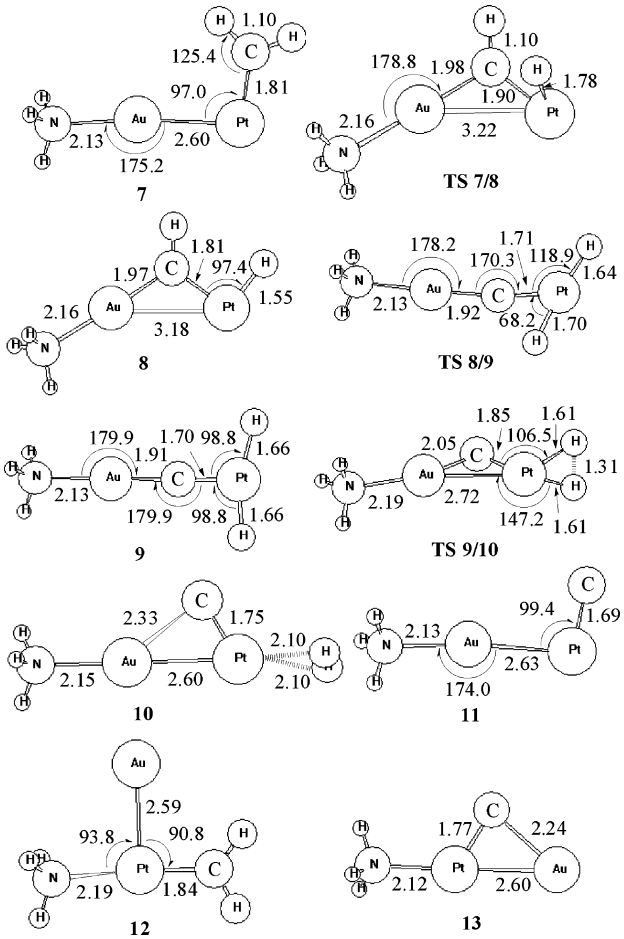

Figure 5. B3LYP-optimized structures of selected intermediates and transition states corresponding to Figure 4 (bond lengths in angstroms and bond angles in degrees).

mol^{-1}, yielding the stable complex **7**. Like complex **1**, strong donor−acceptor interactions are responsible for the Au−N bond in **7**, where NH_3 behaves as a donor and the PtAu subunit behaves as an acceptor. Complex **7** is converted into **8** through a hydrogen shift from C to Pt with a barrier of 31.8 kcal mol^{-1}, which is higher than the hydrogen transfer barrier in **1** by ∼10 kcal mol^{-1}, as shown in Figure 2. This relatively high barrier can be ascribed to a closed-shell bimetallic core $PtAu^+$. The subsequent hydrogen transfer results in **9** with a

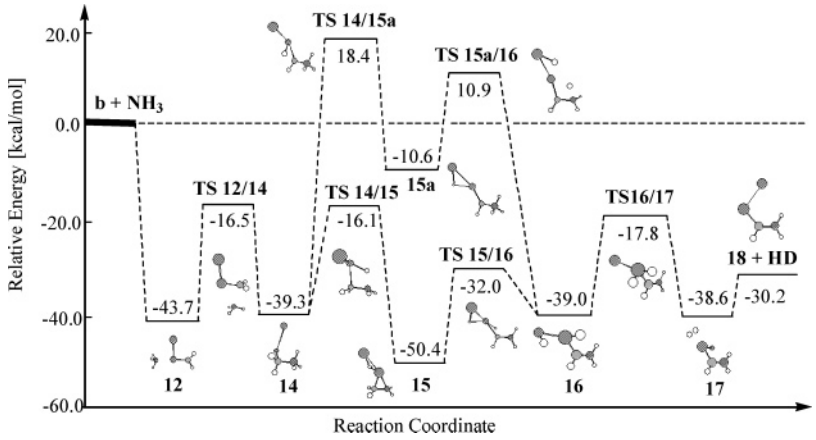

Figure 6. Singlet potential energy profiles along the pathway to loss of H_2 from the stepwise N−H and C−H activation in the complex $(NH_3)PtAuCH_2^+$.

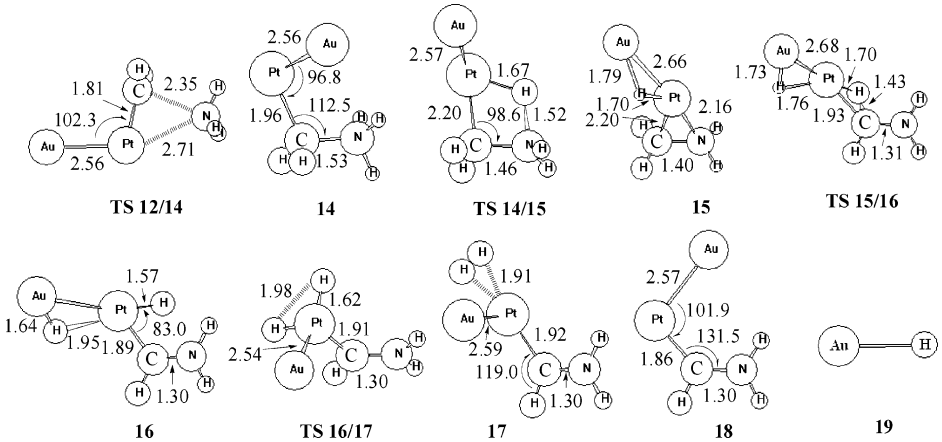

Figure 7. B3LYP-optimized structures of selected intermediates and transition states corresponding to Figure 6 (bond lengths in angstroms and bond angles in degrees).

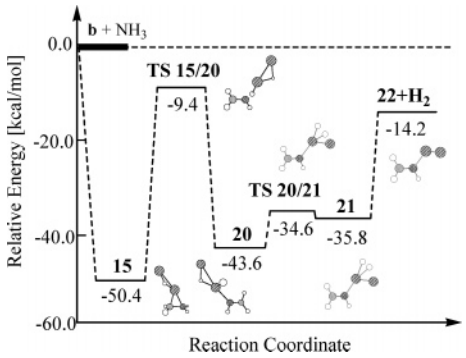

Figure 8. Singlet potential energy profiles along the pathway to loss of H_2 from NH_3 activation mediated by $PtAuCH_2^+$.

barrier of 33.8 kcal mol^{-1}. Association of two hydrogen atoms in **9** gives the dihydrogen complex **10**. This process is endothermic by 18 kcal mol^{-1}. The elimination of D_2 from **10** leads to the ion product **11**, requiring an energy of 2.4 kcal mol^{-1}. As Figure 4 and Table 1 show, the overall reaction has an endothermicity of 8.6 kcal mol^{-1} and free energies of reaction ΔG of 7.1 kcal mol^{-1}(298.15 K).

Similarly, NH_3 attacks the central Pt in $PtAuCD_2^+$ to form complex **12** (Figure 5) with an exothermicity of 43.7 kcal mol^{-1}. Nevertheless, calculations indicate that **12** evolves into ultimate product **13** through dehydrogenation and consecutive reactions with substantially high energies of ~60 kcal mol^{-1}, and it seems not to take place in the gas-phase reaction. Complex **12** as a precursor to loss of HD can be involved in subsequent reactions (vide infra).

Loss of HD. The detailed mechanism and relative energetics for the loss of the HD in the reaction of $PtAuCD_2^+$ with NH_3 are shown in Figure 6. Selected optimized structures of relevant species in the reaction are collected in Figure 7. NBO analyses indicate that the N−Pt bond in **12** arises from strong donor−acceptor interactions of the lone pair of NH_3 with an antibonding orbital of the PtC subunit. The N−C bond coupling through migration of NH_3 to C produces the intermediate **14** with a barrier of 27.2 kcal mol^{-1}. The intermediate **14** isomerizes into **15** with a barrier of 23.2 kcal mol^{-1}, where the N−H bond activation is involved. DFT calculations reveal that the H shift from methylene to Pt in **14** has a quite high barrier of 57.7 kcal mol^{-1}. Therefore, this step via **TS 14/15a** could not occur prior to the H transfer from NH_3 to the bimetallic core. The intermediate **15** is the global minimum in the reaction process, where Au−H and Pt−H bond lengths are 1.79 and 1.70 Å, respectively. It is a typical η^2-H bridged compound. **15** undergoes subsequent H shift from methylene to Pt and H−D association to produce the dihydrogen complex **17**. Complex **17** requires energies of 8.4 kcal mol^{-1} to dissociate into **18** and HD. The metal cationic aminocarbene **18** has a planar structure in which the Pt and C atoms adopt approximately respec-

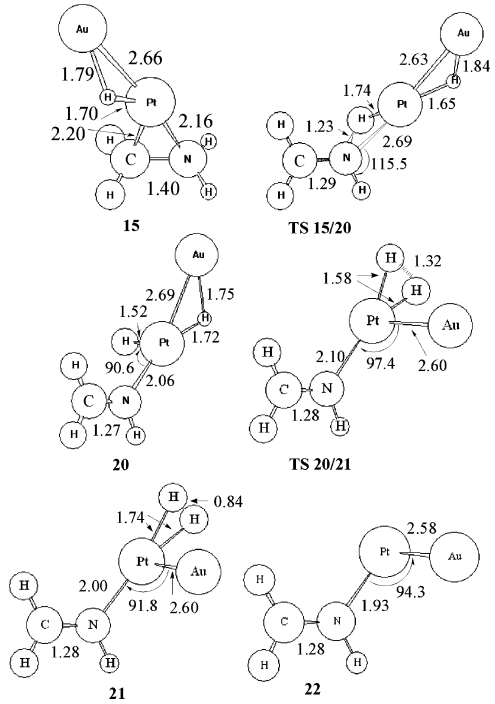

Figure 9. B3LYP-optimized structures of selected intermediates and transition states corresponding to Figure 8 (bond lengths in angstroms and bond angles in degrees).

tive sd^2 and sp^2 hybrid orbitals to bond together. The aminocarbene **18** with high stability can be assigned to a main form of the ion product $[Pt,Au,C,H_2,D,N]^+$ in experiment.[9c]

The overall reaction for the HD loss is exothermic by 30.2 kcal mol^{-1}, and the corresponding free energies of reaction ΔG (298.15 K) are −33.1 kcal mol^{-1}. In comparison with the D_2 elimination, the HD channel is much more favored both thermodynamically and dynamically. This is comparable with the experimental gain for D_2 and HD in a ratio of 70(±15):100.[9a,c]

Loss of H_2. Experimentally, the channel to loss of H_2 in the reaction of $PtAuCD_2^+$ with NH_3 was observed.[9c] This fact shows that NH_3 can afford the dehydrogenation in the case of the $PtAuCD_2^+$ cluster. On the basis of calculations, the plausible mechanism for this channel is proposed in Figure 8. Corresponding structures in the reaction path are given in Figure 9.

As Figure 6 shows, the first dehydrogenation step prefers NH_3 activation to C−H bond activation in the loss of HD. The stable intermediate **15** can serve as a precursor to the second dehydrogenation of ammonia. DFT energetics shown in Figure 8 reveals that the intermediate **15** surmounts a barrier of 41.0 kcal mol^{-1} to give the isomer **20**. The IRC calculations indicate that the cleavage of a strong C−Pt bond ($D_0(Pt^+-CH_2) = 113$ kcal mol^{-1})[4f] is involved in the second N−H bond activation. The intermediate **20** proceeds to the dihydrogen complex **21** with a barrier of 9 kcal mol^{-1}. **21** requires an energy of 21.6 kcal mol^{-1} to lose H_2, giving **22** as a possible form of the ion product $[Pt,Au,C,H,D_2,N]^+$. The overall reaction to products **22** + H_2 has an exothermicity of 14.2 kcal mol^{-1} and free energies of reaction ΔG of −18 kcal mol^{-1} (298.15 K).

Combining relative energies and barriers displayed in Figures 4, 6, and 8, as well as thermodynamic values listed in Table 1, the channel to loss of HD by dehydrogenating both methylene and ammonia is the most favored route for dihydrogen elimination in reaction 3. The next one is the loss of H_2 from NH_3 activation. This accords approximately with the experimental characterization of dihydrogen products D_2, HD, and H_2 in a ratio of 70(±15): 100: 80(±15).[9a,c]

IV. Reactions of $[Pt,Au,C,H_3,N]^+$ and NH_3. Experimentally, the consecutive reactions 4 and 5 of the ionic product $[Pt,Au,C,H_3,N]^+$ with a second NH_3 under loss of H_2 or degradation of the metal core were observed.[9a] To gain insight into these consecutive reactions, we investigated the reaction of the ionic product with a second NH_3 by DFT calculations. As mentioned above, the structure **18** is the most stable candidate among the possible ionic products $[Pt,Au,C,H_3,N]^+$. The stable aminocarbene species **18** has an unsaturated Pt site, which can bind NH_3. Figure 10 displays the relative energy diagram along a possible reaction path to loss of H_2 and AuH. Optimized geometries of intermediates and transition states involved in the reaction are shown in Figure 11.

As shown in Figure 10, coordination of NH_3 to **18** releases an energy of 31.8 kcal mol^{-1}, forming complex **23**. In **23**, the C−N coupling via **TS 23/24** leads to the intermediate **24** with a barrier of 36.5 kcal mol^{-1}. The less stable intermediate **24** proceeds to **25** via NH_3 activation with a barrier of 19.8 kcal mol^{-1}. Followed by C−H bond activation, **25** converts into the intermediate **26**. In **26**, the Au−H, Pt−H, and Au−Pt bond lengths are 1.65, 1.90, and 2.80 Å, respectively. This geometrical feature indicates that elimination of the

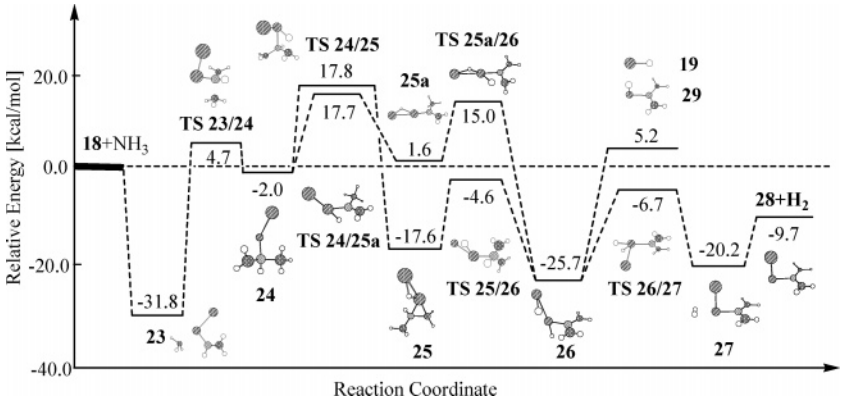

Figure 10. Singlet potential energy profiles along the pathway to loss of H_2 and AuH in the reaction of the aminocarbene $AuPtCHNH_2^+$ with NH_3.

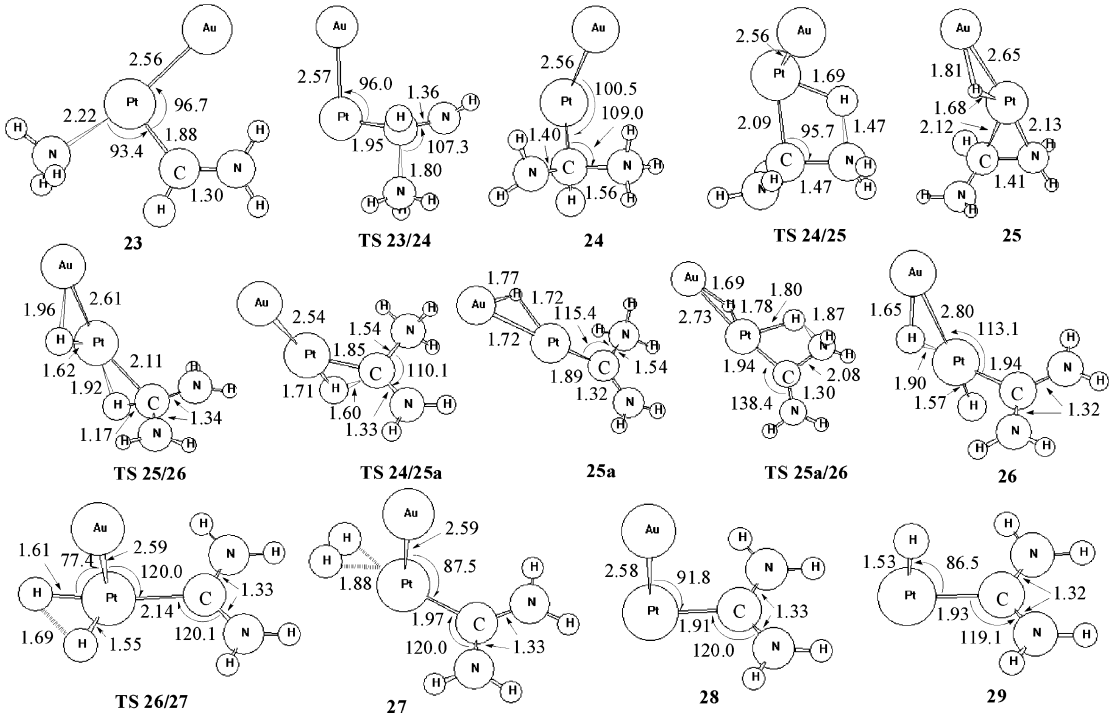

Figure 11. B3LYP-optimized structures of selected intermediates and transition states corresponding to Figure 10 (bond lengths in angstroms and bond angles in degrees).

hydride AuH in **26** can take place in the gas-phase reaction. On the other hand, **26** can be formed through C−H activation in **24** first, followed by N−H activation in **25**. As Figure 10 shows, this process is less favored dynamically. The H−H coupling in **26** gives the dihydrogen complex **27** with a barrier of 19 kcal mol^{-1}. The dihydrogen complex **27** requires an energy of 10.5 kcal mol^{-1} to lose H_2, giving the biaminocarbene product **28**. The biaminocarbene **28** can be assigned as a candidate for the ionic product $[Pt,Au,C,H_4,N_2]^+$ in experiment.[9a]

Concluding Remarks

The structures, stabilities, and relative energies of possible intermediates, transition states, and ionic products for the gas-phase reactions of $PtMCH_2^+$ (M = Pt, Au) with NH_3 have been determined by DFT calculations. On the basis of theoretical calculations, the mechanistic details for dehydrogenation and C−N coupling have been explored. Calculations show that the doublet $Pt_2CH_2^+$ has a ring structure **c** in its ground state $^2A_2$, while the singlet $PtAuCH_2^+$ exists in two isoenergetic isomers, **b** and **d**. Such differences in geometrical and electronic structures play an important role in determining their reactivities. The most stable isomer, **c**, of $Pt_2CH_2^+$ binds NH_3 to form a stable complex, $(NH_3)Pt_2CH_2^+$ (**1**), which undergoes consecutive isomerizations to yield $(NH_3)Pt_2C^+$ and H_2. The overall reaction is exothermic by 10.7 kcal mol^{-1} relative to the reactants **c** and NH_3. The ionic product $(NH_3)Pt_2C^+$ can be stabilized by adduction of a second NH_3, giving an inactive $(NH_3)_2Pt_2C^+$ without occurrence of NH_3 activation.

In the case of the heteronuclear bimetallic carbene $PtAuCH_2^+$, predicted relative energetics and activation energies reveal that the dehydrogenation channels through C−H and N−H activation are competitive and the C−N bond coupling occurs in the consecutive reactions. The ionic product aminocarbene $AuPtCHNH_2^+$ (**18**) can react with a second NH_3, resulting in loss of H_2 and degradation of the metal core, where the overall channel to H_2 is exothermic by 9.7 kcal mol^{-1}, while the route to AuH is endothermic by 5.2 kcal mol^{-1}. Predicted free energies of reaction ΔG (298.15 K) for loss of H_2 and AuH are −11.6 and 0.8 kcal mol^{-1}, respectively. The rate-determining step of the C−N coupling in both channels has a barrier of 46.5 kcal mol^{-1}. Present calculations show reasonable agreement with the experimental observations and provide a basis for understanding reactivities and mechanisms of dehydrogenation and C−N coupling from reactions of bimetallic carbenes $PtMCH_2^+$ (M = Pt, Au) with NH_3.

Acknowledgment. We acknowledge financial support from the National Science Foundation of China (Project Nos. 20173042, 20233020, 20473062, and 20021002), the Ministry of Education of China, and the Ministry of Science and Technology.

OM0490942